Optical and Electron-Spin-Resonance Spectra of Yb^{3+}, Nd^{3+}, and Cr^{3+} in $LiNbO_3$ and $LiTaO_3$†

GERALD BURNS,* D. F. O'KANE, AND REUBEN S. TITLE

IBM, Watson Research Center, Yorktown Heights, New York

(Received 10 October 1967)

The results of optical-spectroscopic and electron-spin-resonance (ESR) studies of Yb^{3+}, Nd^{3+}, and Cr^{3+} impurities are presented. The spectra of Yb^{3+} are discussed in detail. Crystal-field parameters are obtained to fit the energy levels and the ESR results on the ground state. These parameters are not obtained by a least-squares fit but rather by physical considerations as to where, on the threefold axis, the ion could be to give crystal-field parameter ratios that can be used to fit the experimental results.

INTRODUCTION

IN the quantum electronics field, $LiNbO_3$ and $LiTaO_3$ are interesting crystals because they can be used for a variety of purposes.[1] Their large optical nonlinearities, excellent piezoelectric properties, and linear electro-optic coefficients make them good candidates for modulation, deflection, and harmonic experiments.

We have recently found[2] that these compounds can be readily doped with rare earths and transition-metal ions. The resultant energy levels in general are similar to those normally found for the ions. The rare-earth emission is sharp and efficient.

In this paper some results of optical-spectroscopic and electron-spin-resonance (ESR) studies are presented. In particular, the results for Yb^{3+} ($4f^{13}$) are discussed in detail. This ion was chosen because of its relatively simple energy-level diagram (one hole in a $4f$ shell). Crystal-field parameters are obtained to fit the observed energy levels and the ESR results on the ground state. These results are used to try to determine whether the rare earths replace the Li^{1+} or Nb^{5+} ions in the lattice. ESR and optical results are also presented for several other ions in these lattices.

EXPERIMENTAL

The doping of $LiNbO_3$ and $LiTaO_3$ with rare-earth ions was expected to be difficult because the closely related perovskites ($KTaO_3$, $BaTiO_3$, etc.) with similar charges cannot be easily doped. Although some of these perovskites have been doped for ESR measurements, it is very unusual for sharp, efficient photoemission to result. However, we have found that both $LiNbO_3$ and $LiTaO_3$ can be readily doped.

Single crystals of doped $LiNbO_3$ and $LiTaO_3$ were grown by the Czochralski method.[3] The compounds were prepared from stoichiometric quantities of Li_2CO_3 (99.99%), Nb_2O_5 (99.9%), and Ta_2O_5 (99.9%). The $LiNbO_3$ crystals were pulled from a melt containing 0.5 wt. % of Yb_2O_3 and 100 ppm by weight of Cr_2O_3. The $LiTaO_3$ was grown from a melt containing 0.3 wt% of Yb_2O_3 and 50 ppm by weight of Cr_2O_3. Other crystals with widely varying concentrations of impurities were also pulled with the same results.

RESULTS

The space group of $LiNbO_3$ is C_{3v}^6. Both Li^{1+} and Nb^{5+} ions lie on the C_{3v} axis.[1(c),(e)] These ions are thus in a field of axial symmetry and there is no center of inversion in the crystal. Thus the absorptive and fluorescent transitions are expected to be electric dipole in character and there should be no difficulty in determining the true electronic energy levels as has sometimes been the case in, for example, the garnets.[4] The excellent agreement between the results on the absorption and the fluorescence of Yb^{3+} in $LiNbO_3$ and $LiTaO_3$ shows that the pure electronic levels are indeed being measured. The ESR measurements for Yb^{3+}, Nd^{3+}, and Cr^{3+} show that the ions are in a field of axial symmetry. Thus, these ions lie on the C_{3v} axis. The charge compensation appears to be nonlocal.

Figure 1 shows both a sketch of the $LiNbO_3$ crystal structure with[1(c)] the Li and Nb ions between planes of O^{2-} atoms and also a model of the rare-earth ion in an octahedron of six O^{2-} ions. This model will be used

† Preliminary accounts of some of this work has appeared in Bull. Am. Phys. Soc. **12**, 61 (1967); **12**, 358 (1967).

* Partially supported by Army Research Office, Durham, N.C. under Contract DA-31-124-ARO-D-205.

[1] There are many papers on $LiNbO_3$. The following have references to most of them. (a) K. Nassau, H. J. Levinstein, and G. M. Loiacono, J. Phys. Chem. Solids **27**, 983 (1966); (b) *ibid.* **27**, 989 (1966); (c) S. C. Abrahams, J. M. Reddy, and J. L. Bernstein, *ibid.* **27**, 997 (1966); (d) S. C. Abrahams, *ibid.* **27**, 1013 (1966); (e) S. C. Abrahams, H. J. Levinstein, and J. M. Reddy, *ibid.* **27**, 1019 (1966).

[2] G. Burns, D. F. O'Kane, and R. S. Title, Phys. Letters **23**, 56 (1966).

[3] A. A. Ballman, J. Am. Ceramic Soc. **48**, 112 (1965). In this paper the addition of Nd^{3+} and Pr^{3+} is reported to produce fluorescence at frequencies somewhat different from those normally observed. We see no confirmation of this and see the emission and absorption at the usual frequencies.

[4] R. A. Buchanan, K. A. Wickersheim, J. J. Pearson, and G. F. Hersmann, Phys. Rev. **159**, 245 (1967); *ibid.* **159**, 251 (1967); W. P. Wolf, J. Chem. Phys. **41**, 617 (1964). See also J. A. Koningstein and J. E. Geusic, Phys. Rev. **136**, A711 (1965).

later to obtain ratios of the crystal-field parameters. For a rare-earth ion in C_{3v} symmetry, there are six crystal-field terms[5,6]:

$$V=B_2^0(3z^2-r^2)+B_4^0(35z^4-30z^2r^2+3r^4)+B_4^3z(x^3-3xy^2)+B_6^0(231z^6-315z^4r^2+105z^2r^4-5r^6)+B_6^3(11z^3-3zr^2)(x^3-3xy^2)+B_6^6(x^6-15x^4y^2+15x^2y^4-y^6). \quad (1)$$

For Yb^{3+} ($4f^{13}$) in C_{3v} symmetry the ground state $J=\frac{7}{2}$ manifold is completely split into four Kramers doublets. Similarly, the first excited $J=\frac{5}{2}$ state is split into three Kramers doublets. Figures 2 and 3 show the absorption spectra for Yb^{3+} in $LiNbO_3$ and $LiTaO_3$. As can be seen, the low-temperature spectrum consists of three lines with associated vibrational structure. The

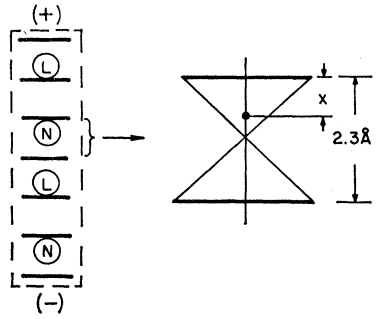

FIG. 1. A sketch of the $LiNbO_3$ crystal structure looking perpendicular to the c axis. The horizontal thick lines represent a triangle of oxygen atoms. L represents the approximate position of the Li ion; N represents the approximate position of the Nb ion. This clearly would be polarized up as shown in the figure [Ref. 1(e)]. The right-hand part of the figure represents a model that will be discussed later. x is the distance between a test charge ion and one of the planes of oxygen ions. The planes of oxygen ions are separated by 2.3 Å [Ref. 1(c)].

sharp line in $LiNbO_3$ at 9802 Å (~8 Å wide at low temperatures) corresponds exactly to the inverse line observed in fluorescence as can be seen in Fig. 4. The results are similar for $LiTaO_3$ where the line appears at 9800 Å. The fluorescence is shown in Fig. 5. The absorption line in Fig. 2 at 1.005 μ that decreases in intensity as the temperature is lowered and completely disappears at 4.2°K corresponds to the 1.0050 μ line observed in fluorescence. Thus it corresponds to absorption from the Kramers doublet above the ground state in the $J=\frac{7}{2}$ manifold to the lowest doublet of the $J=\frac{5}{2}$ level. A similar result can be seen in the $LiTaO_3$ data. The absorption and fluorescence data are consistent and yield the energy levels of the Yb^{3+} ions at least within the accuracy of the uncertainty due to

[5] K. W. H. Stevens, Proc. Phys. Soc. (London) **65A**, 209 (1952).
[6] B. R. Judd, Proc. Roy. Soc. (London) **227A**, 552 (1955); **241A**, 122 (1957).

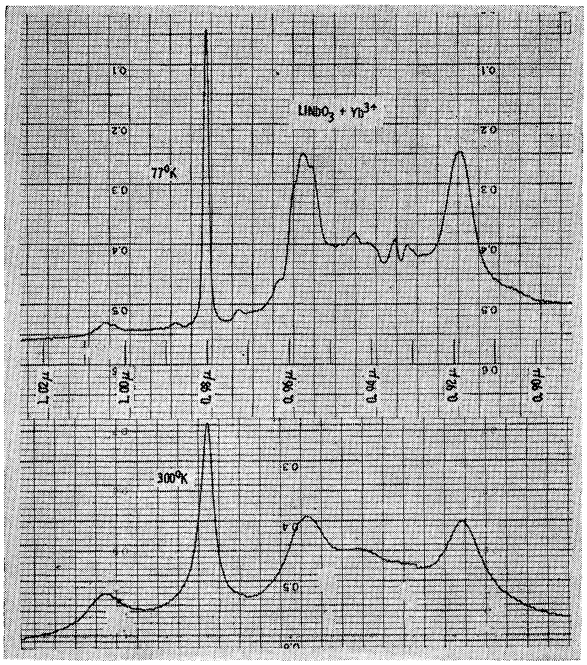

FIG. 2. The absorption spectra of Yb^{3+} in $LiNbO_3$. Absorption data at 4.2°K is very similar to the 77°K data except as discussed in the text. (The data were taken on a dual beam Cary 14 instrument.)

phonon sideband effects. These phonon effects are somewhat similar for the two compounds as can be seen in Figs. 2–5. The 9565 Å line in absorption and the 1.0050 μ line in fluorescence are very similar in that they both look like an "unresolved triplet." This structure can be made much more apparent than shown in the figures under higher resolution, i.e., narrower

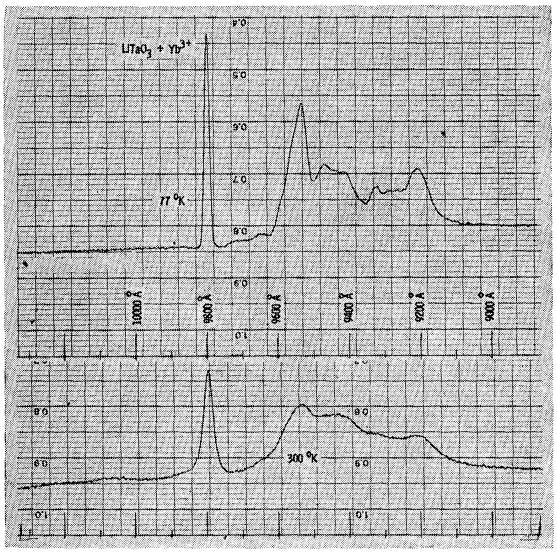

FIG. 3. The absorption of Yb^{3+} in $LiTaO_3$. Comments in figure caption 2 are also apropos to this figure.

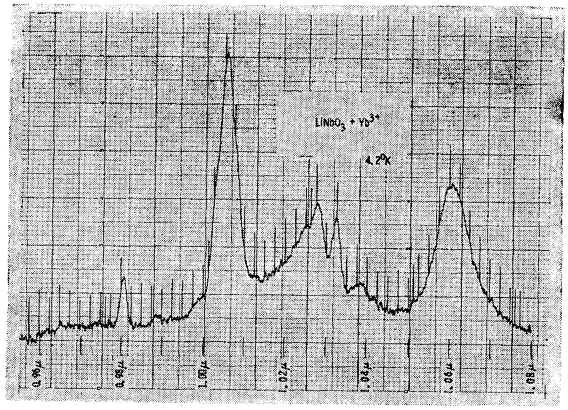

FIG. 4. Fluorescence of Yb^{3+} in $LiNbO_3$. Data taken at 77°K is essentially the same as shown in the figure. However, at room temperature the emission is much broader and loses much of its structure, as can be seen in the next figure.

slits, slower scan, and more time constant. Both of these lines correspond to the first electronic level above the ground state in the $J=\frac{5}{2}$ and $\frac{7}{2}$ manifold, respectively.

The Cr^{3+} absorption in $LiTaO_3$ is similar to that observed in $LiNbO_3$. However, the sharp line, apparently from the ^2E state, occurs at 7165 Å in $LiTaO_3$ and one cannot resolve the doublet. The half-width (full width at half-intensity) is 17 Å, so the doublet must be more closely spaced. Cr^{3+} in both compounds has a broad fluorescence[2] which starts where the absorption ends (~7600 Å) and peaks at ~0.9 μ with a half-width ~0.2 μ. Similar fluorescence has been observed[7] in other compounds containing Cr^{3+}. It is attributed to a Stokes shifted emission from the $^4T_2$ level to the ground state. It is interesting to note the effect this emission has in enhancing the Yb^{3+} emission. The results in Figs. 4 and 5 are both from crystals that were codoped with Cr^{3+}. It was found that this greatly enhanced the Yb^{3+} emission although no change in the positions of the Yb^{3+} levels was observed. At least part of this Yb^{3+} enhancement is due to direct absorption of the broad Cr^{3+} emission by the Yb^{3+} ions, as has been pointed out to us by Welber.[8] This can be seen in Fig. 5: There is a slight dip in the emission near 0.953 μ, which just corresponds to a Yb^{3+} absorption line as can be seen from Fig. 3. The Cr^{3+} emission in this region of the spectra can be observed under much higher signal-to-noise conditions and the Yb^{3+} absorption spectrum can be traced out in complete detail. It is not known if this is the only way that the Cr^{3+} enhances the Yb^{3+} emission.

The Nd^{3+} emission near 1.08 μ in $LiTaO_3$ is similar to that observed[2] in $LiNbO_3$, as are the 0.9 μ and 1.35 μ emissions also. The emissions at 1.08 μ and 1.35 μ have some semiresolved weaker lines on their long-wavelength sides (see the figure in Ref. 2). Except for these lines, the positions of the Nd^{3+} lines in $LiNbO_3$ give energy levels for the three lowest-lying J manifolds of the ^4I levels at: $J=\frac{9}{2}$, 0, 157, 439, and 488: $J=\frac{11}{2}$, 1988, 2040, and 2105: $J=\frac{13}{2}$, 3922, 3974, and 4037, all in cm^{-1}. As mentioned above, both the $J=\frac{11}{2}$ and $J=\frac{13}{2}$ states have unresolved levels at higher energies. However, a crystal field fit to the Nd^{3+} levels was not undertaken and they will not be discussed further.

ESR measurements were made on Yb^{3+} in $LiNbO_3$. The measured parameters are given in Table I. Also included are parameters measured for Cr^{3+} and Nd^{3+} in $LiNbO_3$ and $LiTaO_3$. All ions were observed to be at sites with axial symmetry, with the axis coincident with the trigonal axis of the crystal. In agreement with the optical results, each ion was observed in only one site. The ESR measurements on Yb^{3+} were on the lowest lying Kramers doublet of the $^2F_{7/2}$ ground state while on Nd^{3+} they were on the lowest doublet of the $^4I_{9/2}$ state. In the case of Cr^{3+} the axial field splits the lowest-lying quartet into two doublets characterized by the splitting $2D$. In both $LiNbO_3$ and $LiTaO_3$ we found the splitting $2D$ to be larger than the microwave quantum energy $h\nu$ at X-band. The only allowed transition involves the lowest doublet. The effective g values for this doublet observed under conditions for which $h\nu \ll 2D$ are given by[9] $g_{||}{}^{\text{eff}}=g$ and $g_{\perp}{}^{\text{eff}}=2g[1-3/16(h\nu/2D)^2]$. The g values and the D values calculated from them are given in Table I. In addition to this resonance a number of transitions normally forbidden in first order[10] were also observed.

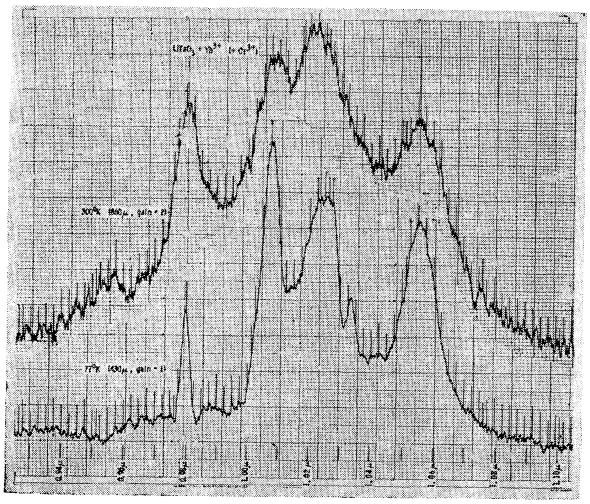

FIG. 5. Fluorescence of Yb^{3+} in $LiTaO_3$. The results at 4.2°K are essentially the same as those shown at 77°K.

[7] A. Misu, J. Phys. Soc. Japan **19**, 2260 (1964); P. Kisliuk and C. A. Moore, Phys. Rev. **160**, 307 (1967); J. H. Parker, Jr., R. W. Weinert, and J.G. Castle, Jr. (to be published).

[8] B. Welber (private communication).

[9] J. E. Geusic, M. Peter and E. O. Schulz-duBois, Bell System Tech. J. **38**, 291 (1959).

[10] E. O. Schulz-duBois, Bell System Tech. J. **38**, 271 (1959).

The ESR lines for each of the ions studied were relatively broad, 50 Oe or wider, and did not vary in width as the temperature was changed. The broadening is probably due to strains caused by incorporation of the impurity ions in the lattice.

The ESR data show that the impurity ions lie on the C_{3v} axis. The position on the axis is not however obtainable from the ESR or optical data alone. To obtain further information concerning the position of the impurity ion, it was decided to perform crystal-field calculations as described in the next section.

DISCUSSION

The object in fitting the Yb^{3+} spectra was to obtain information on the location of the rare-earth ion along the C_{3v} axis. Equation (1) shows that six crystal-field parameters are involved for $4f$ electrons in C_{3v} symmetry. One could vary all of these parameters and get a least-squares fit. This is the usual procedure with rare-earth spectra. However, in our case, it is uncertain if the position of the Yb^{3+} ion could also be obtained from the resulting parameters. Thus, the problem was approached from a more physical point of view by use of a method that would yield the position of the Yb^{3+} ion immediately. The details of this approach are outlined below.

In Fig. 1 it can be seen that both the Li and Nb ions lie on the C_{3v} axis surrounded by six O^{2-} ions which are arranged in two planes separated by 2.3 Å at room temperature. We assumed that the rare-earth ions are on the C_{3v} axis a distance x from one plane of oxygen ions and a distance (2.3 Å$-x$) from the other. The model we have chosen for the calculations will therefore determine the position of the rare-earth relative to the oxygen planes. A range of x was chosen so that the origin would pass through a Li^{1+} position which is $\approx$0.7 Å from the nearest origin and also the Nb^{5+} position $\approx$0.9 Å from its nearest oxygen plane. A reasonable approach is to keep the rare-earth–oxygen internuclear-distance constant, independent of x. Thus, as the rare-earth ion approaches the oxygen triangle, that triangle increases in area while the triangle that is farther away from the rare earth is reduced. This can be seen in (b) of Fig. 1. The last problem to consider

TABLE I. The resonance parameters for Yb^{3+}, Cr^{3+} and Nd^{3+} in $LiNbO_3$ and $LiTaO_3$.

	$LiNbO_3$		$LiTaO_3$	
	$g_{\|\|}$	$g_\perp$ ($g_\perp^{eff}$)	$g_{\|\|}$	$g_\perp$ ($g_\perp^{eff}$)
Yb^{3+}	4.86	2.69		
Cr^{3+}	1.969	(3.870)	1.971	(3.863)
	$D=0.45\pm0.05$ cm^{-1}		$D=0.43\pm0.05$ cm^{-1}	
Nd^{3+}	1.42	2.94		

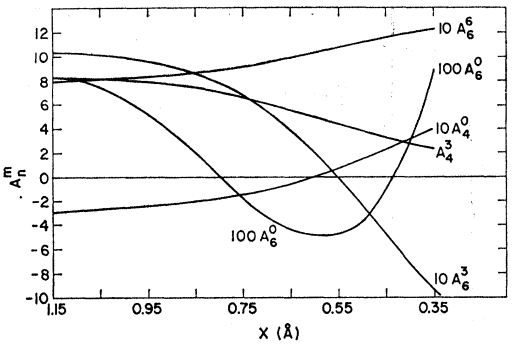

FIG. 6. A plot of A_n^m versus x. x is defined in the text and in Fig. 1.

before lattice sums can be calculated is the internuclear distances to be used. A normal rare-earth–O^{2-} internuclear distance is $\approx$2.4 Å. If that were used for this problem the distance between the oxygen planes clearly would have to be changed. A more appropriate rare-earth–O^{2-} distance to use for the $LiNbO_3$ cell is 1.99 Å, which is also the average of the two Nb–O distances in the lattice.[1(c)]

Lattice sums A_n^m, directly related to the coefficients in Eq. (1), were calculated as a function of x for only the oxygen nearest neighbors and the results are in Fig. 6. These A_n^m's (see Ref. 11) have the same signs as the B_n^m's in Eq. (1) and only differ from them by $\langle r^n \rangle$ and physical constants. To calculate these sums only the nearest neighbors were used for several reasons. It is not clear how the rest of the lattice will relax as x is varied, and we feel that the introduction of additional less justified assumptions would reduce the validity of the calculations. Also, only the ratios of the various lattice sums were used. A certain amount of inaccuracy could be tolerated since it should tend to cancel out. However, most important, only the $n=4$ and 6 sums were used and for these the nearest oxygen ions usually make up most of the contribution.[12]

To actually fit the energy levels of Yb^{3+} and g values various guesses for B_4^0 and B_6^0 were made independent of x. The other values dependent on x were selected as follows: $B_4^3=(A_4^3/A_4^0)B_4^0$ and $B_6^m=(A_6^m/A_6^0)B_6^0$ so that only the ratios of the lattice sums were used.[13] For a given set of B_4^0 and B_6^0 the energy levels and g values were calculated as a function of x for $x=1.15$ to 0.35 Å. This was done on an IBM-7094 for steps of $x=0.05$.

[11] The lattice sum A_n^m's are defined below. These sums are summed over only two values of the angle, one for the atom in the plane above and one in the plane below. The other atoms are already taken care of in numerical factor. $A_2^0=(3/4)\Sigma[3\cos^2\theta-1]$; $A_4^0=(3/64)\Sigma[35\cos^4\theta-30\cos^2\theta+3]$; $A_4^3=(105/8)\Sigma[\cos\theta(1-\cos^2\theta)^{3/2}]$; $A_6^0=(3/356)\Sigma[231\cos^6\theta-315\cos^4\theta+105\cos^2\theta-5]$; $A_6^3=(315/128)\Sigma[(11\cos^2\theta-3)(1-\cos^2\theta)^{3/2}]$. As defined, the sign for the A's and B's is the same.

[12] G. Burns, Phys. Rev. **128**, 2121 (1962); E. Y. Wong and I. Richman, J. Chem. Phys. **36**, 1889 (1962); and M. T. Hutchings and D. K. Ray, Proc. Roy. Soc. (London) **81**, 633 (1963).

[13] M. T. Hutchings and W. P. Wolf, J. Chem. Phys. **41**, 617 (1964).

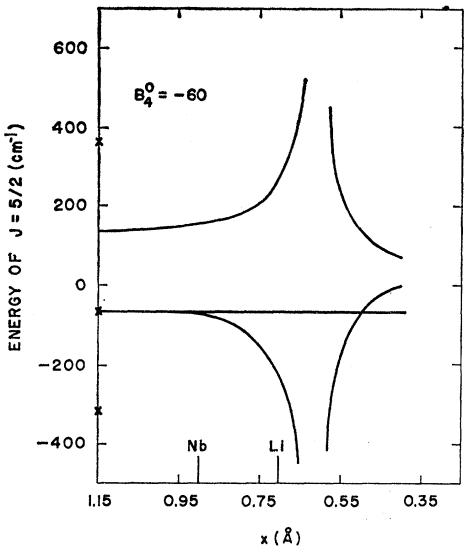

FIG. 7. The energy of the $J=\frac{5}{2}$ level as a function of x for $B_4^0=-60$ cm^{-1}. The experimental data represented by crosses are shown on the left-hand side of the figure. The approximate positions in the unit cell of the Li ion and the Nb ion are shown.

The range of x covers both the Li^{1+} position at $x\approx 0.70$ and the Nb^{5+} position at $x=0.90$.

A further simplification occurs for the Yb^{3+} levels because the $J=\frac{5}{2}$ level can be fitted with only B_4^0 and B_4^3. The effect of the $n=6$ terms on the splittings for this $J=\frac{5}{2}$ level is very small. Also the effect of B_2^0 on this level turns out to be small. Figure 7 shows the energy splittings for this level as a function of x along with the experimental values on the left. As can be seen, a rather good fit is obtained for $x=0.67$ and $B_4^0=-60$ cm^{-1}. The sign of this value of B_4^0 for $x=0.67$ is consistent with the sign of B_4^0 calculated in the lattice sum. (See Fig. 6.) The apparent fit at $x\approx 0.55$ is inconsistent with a negative value of B_4^0 and can only result from a positive value of B_4^0. However, a positive value of B_4^0 would not fit the experimental data since the calculated value of -68 cm^{-1} would then be $+68$ cm^{-1}.

One can then focus attention on the $J=\frac{7}{2}$ level. Again, energy versus x can be plotted, keeping $B_4^0=-60$ cm^{-1}, and choosing several values of B_6^0 with the other B_n^m's determined from ratios of the lattice sums as above. The results are poor mainly because several of the lattice sums go through zero in the region of interest ($x\approx 0.6$ Å) as can be seen in Fig. 6. Thus it is difficult to decide what is happening. The restriction that the ratios for the $n=4$ and the $n=6$ terms be used for the exact same value of x is a rather strict one considering the simplicity of the model with the inclusion of only nearest neighbors with the full O^{2-} charge and no dipole moment. To reduce the restrictions of the model the values of B_4^0 and B_4^3 were held fixed at values that give good results for $J=\frac{5}{2}$ level and the energy recalculated for several choices of the sixth-order parameters. Much better results were obtained. As can be seen in Fig. 8 the calculated energy separations are reasonably close to the experimentally observed ones for the $J=\frac{7}{2}$ level at $x=0.60$ Å. We think that the similarity between this value of x and the above value of $x=0.67$ for the $J=\frac{5}{2}$ level is indicative that the rare-earth ion, or more specifically the Yb^{3+} ion, lies at $x\approx 0.6$ Å. This value is in the neighborhood[1(c)] of $x=0.70$ Å at which the Li^{1+} ion is located in the undistorted lattice. The Nb^{5+} ion is located at $x=0.90$ Å.

The g values were calculated from the parameters that gave the best fit to the optical data. The calculations gave $g_{\|}=1.048$ and $g_{\perp}=0.664$, which are considerably smaller than the values given in Table I. The g values are much more sensitive to the value of x than are the energy levels. In the region around $x=0.6$ where a good fit to the energy separations is obtained the A_6^3 and A_6^0 are varying rapidly and also going through zero in this region. Within the framework of obtaining the B_n^m ($m\neq 0$) from the ratios of lattice sums it is not possible to reproduce the experimental g values and also obtain a reasonable fit to the energy levels. Thus, it was decided to loosen somewhat the restrictions on the ratios of the B_n^m's ($m\neq 0$) and see if a better fit to the g values could be obtained without altering the energy separations too much.

This was done with moderate success. The following set of B_n^m values was settled on: $B_2^0=0$; $B_4^0=-60$; $B_4^3=\pm 5000$; $B_6^0=-50$; $B_6^3=\mp 3800$; $B_6^6=500$ all in cm^{-1}. $B_2^0\neq 0$ either positive or negative did not noticeably improve the fit so we cannot give an estimate of its value. The $\pm$ values for B_4^3 and B_6^3 are as expected.[6] With these values one calculates for the ground state $g_{\|}=4.8$, $g_{\perp}=2.2$, and the average absolute deviation of energy levels is 75 cm^{-1}. The latter value is higher than the energy fit shown in Fig. 7 where a fit to within 15 cm^{-1} instead of 75 cm^{-1} is obtained. The B_n^m values are

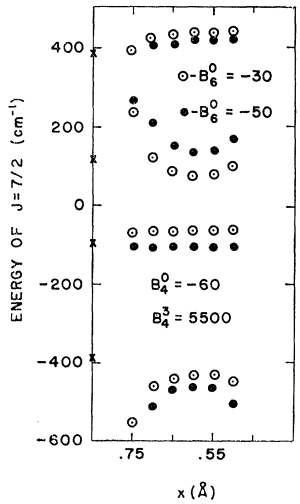

FIG. 8. The energy levels of the $J=\frac{7}{2}$ manifold versus x. For these calculations B_4^0 and B_4^3 were held fixed. The calculations were carried out for two values of B_6^0, namely -30 and -50 cm^{-1}, as can be seen in the figure. The experimental data is shown by crosses at the left-hand side of the figure.

still indicative of the Yb^{3+} occupying a position at $x \approx 0.6$ since it is not hard to move the nearest neighbor to positions that begin to approximate the above ratios.

In summary the fits obtained for the crystal-field split levels of the $^2F_{7/2}$ and $^2F_{5/2}$ states of Yb^{3+} and for the g values of the ground doublet of the $^2F_{7/2}$ state indicate that Yb^{3+} is located at ≈ 0.6 Å from an oxygen plane. While there are several inequivalent positions in the lattice that are 0.6 Å from an oxygen plane the interstitial sites (i.e., those not normally occupied by Li or Nb) are improbable as possible sites for the Yb^{3+} ion since the internal strains would be far too large to accommodate a Yb^{3+} ion at these sites. We believe that the results indicate that Yb^{3+} is most likely substitutional on the Li site but the possibility that it is substitutional on the Nb site with a subsequent relaxation of its position by 0.3 Å cannot be rigorously excluded. Also optical and electron-spin-resonance data is reported for Cr^{3+} and Nd^{3+} in $LiNbO_3$[14] and $LiTaO_3$.

ACKNOWLEDGMENTS

It is a pleasure to thank W. J. Fitzpatrick, B. A. Jenkins, and K. H. Nichols for technical assistance. We also thank A. H. Nethercot for a careful reading of the manuscript and B. Welber for informative discussions.

[14] Laser action of Nd^{3+} in $LiNbO_3$ has been reported. N. F. Evloanova, A. S. Kovalev, V. A. Koptsik, A. M. Prohkorov, and L. N. Rashkovich, Zh. Eksperim. i Teor. Fiz. **5**, 251 (1967) [English transl.: Soviet Phys.—JETP **5**, 291 (1967)].

PHYSICAL REVIEW VOLUME 167, NUMBER 2 10 MARCH 1968

Higher-Shell Contributions and Polarization Correlations in Single-Quantum Annihilation of Positrons

C. V. SHETH* AND N. V. V. J. SWAMY†

Karnatak University, Dharwar, India

(Received 5 July 1967)

It is shown that contribution to the single-quantum annihilation cross section from the $2s_{1/2}$ bound electrons cannot be ignored. Calculations of the cross sections have also been made by applying the Biedenharn-Swamy symmetric model, and the region of validity of this model is estimated. Polarization correlations are studied using Dirac-Coulomb wave functions.

I. INTRODUCTION

EXPERIMENTAL and theoretical studies of single-quantum annihilation of positrons with bound electrons have gained momentum in the past few years.[1] The experimental work reported till now refers to measurement of the cross section as a function of positron kinetic energy and the Z value of the atoms in the solid. After the first nonrelativistic estimate of this cross section by Fermi and Uhlenbeck[2] and the approximate relativistic calculations made several years ago,[3] more refined work has recently been carried out.[4] While Fermi and Bethe take into account the annihilation of positrons with K- and L-shell electrons, Johnson's cross sections are based on ignoring all but the K-shell annihilation.

It has long been known that polarization correlations exist in other electron-photon interactions as a result of their carrying a spin angular momentum. For instance, in the case of bremsstrahlung with polarized electrons, an electron which is longitudinally polarized has a high probability of radiating in the forward direction a circularly polarized high-energy photon with the same helicity.[5] Similarly, there is a preferential ejection of photoelectrons in the plane defined by the momentum and polarization vectors of linearly polarized photons.[6] While electrons are polarized in Coulomb scattering,[7]

* Based in part on a thesis submitted to the Karnatak University for the Ph.D. degree.

† Present address: Department of Physics, Oklahoma State University, Stillwater, Okla.

[1] L. Sodickson, W. Bowman, J. Stephenson, and R. Weinstein, Phys. Rev. **124**, 1851 (1961); H. Langhoff, H. Weigmann, and A. Flammersfeld, Nucl. Phys. **41**, 575 (1963); H. Weigmann, H. Hansen, and A. Flammersfeld, *ibid.* **45**, 555 (1963); M. J. Glaubman, J. D. Oberholtzer, R. Weinstein, and W. P. Crocker, Bull. Am. Phys. Soc. **11**, 121 (1966).

[2] E. Fermi and G. E. Uhlenbeck, Phys. Rev. **44**, 510 (1933).

[3] H. J. Bhabha and H. R. Hulme, Proc. Roy. Soc. (London) **146**, 723 (1934); H. A. Bethe, *ibid.* **150**, 136 (1935); J. C. Jaeger and H. R. Hulme, Proc. Cambridge Phil. Soc. **32**, 158 (1936).

[4] W. R. Johnson, D. J. Buss, and C. O. Carroll, Phys. Rev. **135**, A1232 (1964), hereinafter referred to as R4.

[5] U. Fano, K. W. McVoy, and J. R. Albers, Phys. Rev. **116**, 1159 (1959).

[6] R. H. Pratt, R. D. Levee, R. L. Pexton, and W. Aron, Phys. Rev. **134**, A898 (1964).

[7] N. F. Mott and H. S. Massey, *The Theory of Atomic Collisions* (The Clarendon Press, Oxford, England, 1949).

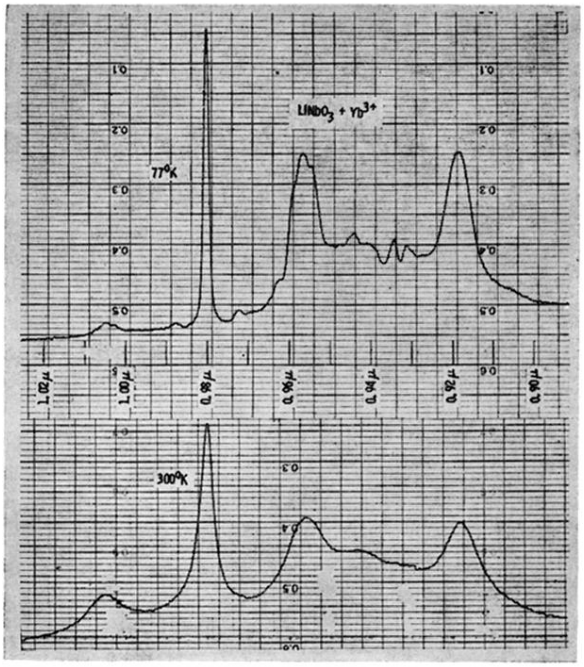

FIG. 2. The absorption spectra of Yb^{3+} in $LiNbO_3$. Absorption data at 4.2°K is very similar to the 77°K data except as discussed in the text. (The data were taken on a dual beam Cary 14 instrument.)

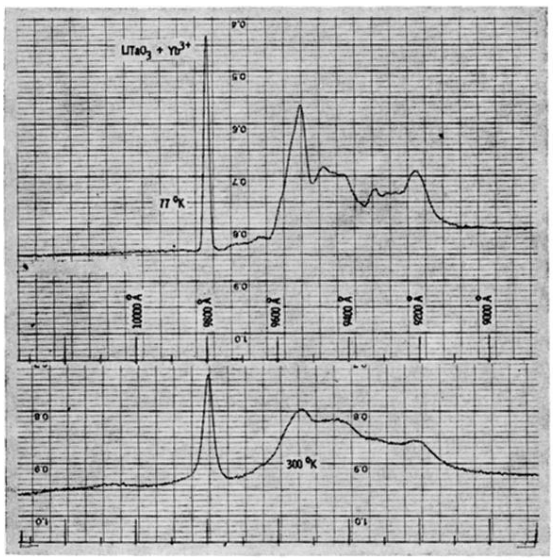

FIG. 3. The absorption of Yb^{3+} in $LiTaO_3$. Comments in figure caption 2 are also apropos to this figure.

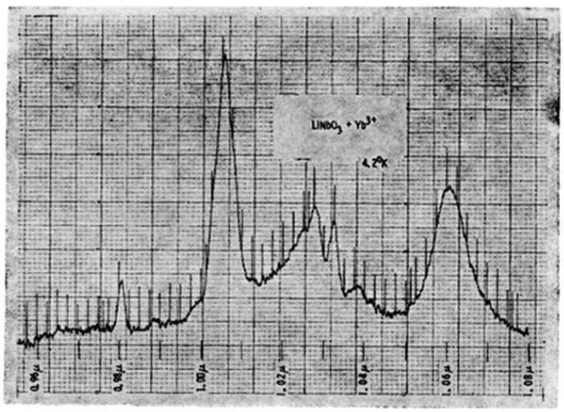

FIG. 4. Fluorescence of Yb^{3+} in $LiNbO_3$. Data taken at 77°K is essentially the same as shown in the figure. However, at room temperature the emission is much broader and loses much of its structure, as can be seen in the next figure.

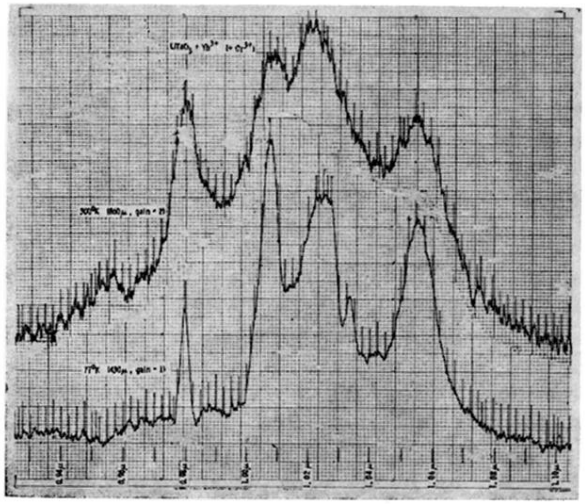

FIG. 5. Fluorescence of Yb^{3+} in $LiTaO_3$. The results at 4.2°K are essentially the same as those shown at 77°K.